

FABRICATION OF ALLOY 625 THROUGH ELECTRON BEAM POWDER BED FUSION
ADDITIVE MANUFACTURING, CHARACTERIZATION AND MECHANICAL
PERFORMANCE

ALDO RUBIO HIDALGO

Master's Program in Mechanical Engineering

APPROVED:

Francisco Medina, Ph.D., Chair

Ryan Wicker, Ph.D.

Amit Lopes, Ph.D.

Stephen L. Crites, Jr., Ph.D.
Dean of the Graduate School

Copyright ©

by

Aldo Rubio Hidalgo

2021

DEDICATION

This thesis is dedicated to my family and everyone who has helped me along my educational and professional path.

PREVIEW

FABRICATION OF ALLOY 625 THROUGH ELECTRON BEAM POWDER BED FUSION
ADDITIVE MANUFACTURING

by

ALDO RUBIO HIDALGO, B.S.M.E.

THESIS

Presented to the Faculty of the Graduate School of
The University of Texas at El Paso
in Partial Fulfillment
of the Requirements
for the Degree of

MASTER OF SCIENCE

Department of Mechanical Engineering
THE UNIVERSITY OF TEXAS AT EL PASO
December 2021

ACKNOWLEDGEMENTS

I would like to extend my gratitude to Dr. Francisco Medina, Associate Professor of the Mechanical Engineering Department and Director of Technology and Engagement at the W.M. Keck Center for 3D Innovation, for giving me the opportunity to put in practice and develop my skills as a Mechanical Engineer in the area of Additive Manufacturing, and for his continuous support and guidance. Additionally, I would like to thank Dr. Ryan Wicker, Director and Founder of the W. M. Keck Center, and all staff members for cultivating an environment of opportunity, growth, and professionalism in the center. Thanks to Dr. Edel Arrieta, Post-Doctoral Research Scholar at the W. M. Keck Center, for his availability, support, and willingness to pass on knowledge of the different systems that are operated in the facility. Finally, I would like to thank lab teammate Mr. Kurtis Watanabe, and Paul Gradl from National Aeronautics and Space Administration (NASA) whose cooperation was crucial for the completion of this project.

ABSTRACT

Electron Beam Powder Bed Fusion (EB-PBF) is an additive manufacturing process that allows for the fabrication of nearly fully dense Alloy 625 parts. In this study EB-PBF Alloy 625 samples were fabricated in an Arcam A2X, heat-treated, then machined and tensile tested. Preliminary process tests varying focus offset, and speed function were conducted to establish baseline process parameter conditions to fabricate Alloy 625 parts based on surface finish and structural defects. The microstructure observed in EB-PBF Alloy 625 parts along the build direction in the as-built state consists of irregularly sized columnar grains averaging 105 μm in width that have formed parallel to the build direction and contain γ'' Ni_3Nb columnar precipitates.

Mechanical properties and microstructures of as-built and heat-treated tensile coupons printed vertically and horizontally were compared. A higher yield strength of 0.387 GPa was observed on as-built horizontally printed parts compared to the vertically printed parts, which produced a yield strength of 0.365 GPa. The presence of anisotropic mechanical properties of parts in the as-built state is attributed to the process-induced columnar microstructure and fusion between layers.

The proposed heat treatment resulted in parts with a relative skeletal density of 99.99%, and a major reduction in internal porosity of approximately 90% %, from 0.52 % to 0.05%, when compared to the as-built parts. Moreover, the heat treatment dissolved the γ'' columnar precipitates and recrystallized the columnar grains into an equiaxed NiCr grain structure with annealing twins in both horizontal and vertical planes. This led to an increase in percent elongation by ~20%, resulting in 69% elongation at fracture. The optimization of process parameters in combination

with the proposed heat treatment allowed for defect reduction and microstructure uniformity in EB-PBF Alloy 625 printed parts, which are of value for end-use application.

PREVIEW

TABLE OF CONTENTS

ACKNOWLEDGEMENTS.....	v
ABSTRACT.....	vi
TABLE OF CONTENTS.....	viii
LIST OF TABLES.....	x
LIST OF FIGURES	xi
CHAPTER 1: INTRODUCTION.....	1
1.1 Motivation.....	2
1.2 Thesis Objectives	2
CHAPTER 2: LITERATURE REVIEW	4
2.1 Binder Jetting.....	4
2.2 Directed Energy Deposition.....	5
2.3 Material Extrusion	6
2.4 Material Jetting	7
2.5 Sheet Lamination	8
2.6 Vat Photopolymerization	9
2.7 Powder Bed Fusion.....	10
2.7.1 Electron Beam Powder Bed Fusion (EB-PBF): EB-PBF Process Characteristics, EB-PBF Workflow & Machine Operation Review	11
2.7.2 PBF Fabrication of Alloy 625: Feedstock and Build Characterization	28
2.7.2.1 Chemical Composition and Feedstock Properties	28
2.7.2.2 Microstructure: EB-PBF.....	30
2.7.2.3 Microstructure: EB-PBF HIP	40
2.7.2.4 Microstructure: Wrought.....	42
2.7.2.5 Microstructure: L-PBF	42
2.7.2.6 Microstructure: L-PBF HIP.....	44
2.7.2.7 Mechanical Properties: EB-PBF	45
2.7.2.8 Mechanical Properties: Wrought and Cast.....	47
2.7.2.9 Mechanical Properties: L-PBF	48

CHAPTER 3: EXPERIMENTAL METHODS	50
3.1 Powder Feedstock Characterization.....	50
3.2 Electron Beam Powder Bed Fusion System	55
3.3 Process Parameter Development.....	55
3.3.1 Speed Function Test.....	56
3.3.2 Focus Offset Test	59
3.4 Heat Treatment.....	65
3.5 Tensile Specimen Preparation.....	66
3.6 Microstructural Characterization	67
3.7 Density and Porosity Measurements.....	68
3.8 Tensile Testing.....	69
3.9 Hardness Testing.....	69
3.10 Fracture Surface Characterization.....	70
CHAPTER 4: RESULTS AND DISCUSSION.....	71
4.1 Microstructural Analysis.....	71
4.2 Mechanical and Physical Properties	74
4.3 Tensile Fracture Surface Analysis	79
CHAPTER 5: CONCLUSIONS	82
REFERENCES	84
APPENDIX.....	96
VITA.....	101

LIST OF TABLES

Table 1. Chemical composition of Alloy 625 wrought product, EB-PBF and L-PBF precursor powders and fabricated components.	29
Table 2. Alloy 625 precursor powder characterization.....	30
Table 3. Process parameters to build porous, well-melted and over-melted samples [5].....	35
Table 4. Mechanical properties of wrought and cast Alloy 625 [70].	47
Table 5. Chemical composition of Alloy 625 powder from Praxair.....	51
Table 6. Process parameters design of experiments for varying speed function and values for skeletal density and internal porosity.....	58
Table 7. Process parameters design of experiments for varying focus offset.....	62
Table 8. Process parameters design of experiments for varying focus offset and values for skeletal density and internal porosity.....	63
Table 9. Optimized process parameters values.....	64
Table 10. Values for microhardness, skeletal part density, percent porosity of as built parts using 50 and 100 μm layer thickness.....	74
Table 11. Values of skeletal density and internal part porosity of heat treated and built parts printed using 50 μm layer thickness.	75
Table 12. Average mechanical properties of heat treated and built parts and their corresponding \pm standard deviation.	75

LIST OF FIGURES

Figure 1. Schematic of binder jetting three-dimensional printing technology [13].	5
Figure 2. Schematics of two DED systems (A) uses laser together with powder feedstock and (B) uses electron beam and wire feedstock [15].	6
Figure 3. Schematic of the material extrusion process [11].	7
Figure 4. Schematic of the material jetting process [30].	8
Figure 5. Schematic of sheet lamination process [37].	9
Figure 6. Components of a typical SLA machine: (1) printed part, (2) liquid resin, (3) building platform, (4) UV laser source, (5) XY scanning mirror, (6) laser beam, (7) resin tank, (8) window, and (9) layer-by-layer elevation [41].	10
Figure 7. Electron Beam Melting (EBM) Mechanism (source www.arcam.com) on the left and 3D schematic of an Arcam A2X EB-PBF machine [49].	11
Figure 8. Arcam build chamber removable parts according to Arcam Q10 and A2X Operations Manual. (1) Front plate, (2) Powder hoppers, (3) Rake flaps, (4) Heat shield [58][60].	15
Figure 9. EBM metallization. Red: top image shows two surfaces around the beam column with metallization; the bottom image shows the surfaces post cleaning. Yellow: the right image shows flaps with metallization; right image shows flaps post fine grinding [58].	16
Figure 10. Removing hopper gates as per Arcam A2X Operations Manual [58].	17
Figure 11. Schematic of manually centered plate according to Arcam A2X Operations Manual [58].	17
Figure 12. Centered and leveled substrate plate on an even powder bed.	18

Figure 13. Outermost rake position calibration according to Arcam A2X Operations Manual [58].	19
Figure 14. Rest rake position calibration on the right and rake flap representation on the left according to Arcam A2X Operations Manual [58].	20
Figure 15. Initial fetch position calibration according to Arcam A2X Operations Manual [58].	20
Figure 16. Left: required distance between powder trigger (1) and powder sensor (2) according to Arcam A2X Operations Manual. Right: using a 2.5 mm hex key to calibrate powder sensor [58].	21
Figure 17. Arcam A2X cleaned and assembled build chamber.	22
Figure 18. Arcam A2X chamber door O-ring.	23
Figure 19. Beam alignment and optimized beam intensity.	24
Figure 20. EB-PBF layer processing steps [4].	26
Figure 21. Employing a powder recovery system (PRS) to extract final part from sintered block.	27
Figure 22. Magnified SEM view of Alloy 625 powder particle showing classical Rapid Solidification Rate (RSR) micro-dendrite structures with optical microscopy image for the corresponding etched cross-section showing the interior microdendritic structure [6].	31
Figure 23. Left: SEM micrographs of initial Alloy 625 powder particles showing a spherical morphology with satellites. Right: [5].	32
Figure 24. Top surface views of samples fabricated by EBM. (a) Typical surface view of porous sample, (b) Well-melted sample, (c) Over-melted sample [5].	32
Figure 25. Process parameter window as a function of Speed Function and Focus Offset suitable for near fully dense parts. White X corresponds to the selected parameters for Inconel 625 [5].	34

Figure 26. Process parameter window suitable for well-melted samples [5].	35
Figure 27. Optical micrographs of EBM samples melted with different beam density. (a) 3mA - Porous, (b) 5mA - Well melted, (c) 12mA - Over melted [5].	36
Figure 28. 3D optical micrograph of manufactured sample with chosen optimal parameters as per [5]. Build direction (BD) is represented by the arrow on the left.	37
Figure 29. Left: IPF orientation map of well-melted sample; Right: EBSD map of porous sample [5]. Build direction (BD) is represented by the arrow on the top right.....	38
Figure 30. Columnar grain width variation along an over-melted sample height [5].....	38
Figure 31. 3D optical micrograph of EB-PBF as-fabricated samples showing columnar precipitate architectures and columnar grain boundaries (GB) containing precipitates. Left [6], Right [71]. Build direction (BD) is represented by the arrow on the bottom right.....	40
Figure 32. Grain structure for HIPed EBM samples. Left: [6]; Right: [71]. Build direction (BD) is represented by the arrow on the bottom right.	42
Figure 33. SEM images of wrought Inconel 625 samples annealed one hour at : (a) 700°C; (b) 900°C; (c) 1100°C [7].....	42
Figure 34. 3D optical micrographs of LPBF as-fabricated fabricated components [71]. Left: Z-axis fabricated component. Right: X, Y- axis fabricated component.	43
Figure 35. L-PBF laser melt scan banding (a) optical microscopy image in vertical reference plane; (b) SEM image showing precipitate/second phase formation within melt bands; (c) Magnified SEM image showing melt-band precipitates [71].	44
Figure 36. Optical microscopy images of HIPed LPBF fabricated samples showing equiaxed, fcc (NiCr) grain structure and associated precipitation. Left: Z-axis fabricated component. Right: X, Y- axis fabricated component [71].	45

Figure 37. Failed tensile sample with SEM image of fractured surface [71].	46
Figure 38. Gas atomization process showing molten metal being poured into a crucible above the atomization chamber (top left). High pressure gas streams disintegrating molten metal (right). Atomization tower (lower left). Courtesy Joe Strauss, HJE Company, Inc [77]......	52
Figure 39. Particle size distribution graph acquired from Retsch Camsizer X2.....	53
Figure 40. Optical microscopy image at 100X magnification showing gas porosity within as received Alloy 625 powder particles.	54
Figure 41. Flowmeter Apparatus – Hall Funnel. Density Cup ($25 \pm 0.03 \text{ cm}^3$) [56].	55
Figure 42. Top surface views of cubic specimens printed with different speed function (SF). ...	57
Figure 43. Schematic illustrating melt pool geometry. Cross-sectional view perpendicular to the direction of beam motion. The melt pool shape for the defocused beam is shallower than that for the focused beam [79].	60
Figure 44. Schematic of melt pool with increased focus offset in EB-PBF process.	60
Figure 45. Top surface views of cubic specimens with different focus offset.	63
Figure 46. Build layout for focus offset test.	64
Figure 47. Schematic of the layout for vertical and horizontally.	66
Figure 48. Optical microscopy images of 50 μm (top) and 100 μm (bottom) layer thickness EB-PBF Alloy 625 as built parts sectioned along the build direction.....	72
Figure 49. Optical microscopy image of heat-treated Alloy 625 part using 50 μm layer thickness.	73
Figure 50. Average tensile mechanical properties of heat treated and built parts with their corresponding \pm standard deviation.	77

Figure 51. Main effects plot for the means of yield strength observed in heat treated (HT) and as built (AB) parts printed horizontally (H) and vertically (V).....	78
Figure 52. Main effects plot for the means of elongation observed in heat treated (HT) and as built (AB) parts printed horizontally (H) and vertically (V).....	79
Figure 53. Scanning electron microscopy (SEM) images of fracture surfaces. (a) and (b) are low and high magnification of an as built vertical sample. (c) and (d) are low and high magnification of a heat-treated vertical sample. (e) and (f) are low and high magnification of an as built horizontal sample.	81

PREVIEW

CHAPTER 1: INTRODUCTION

Alloy 625 is a highly alloyed nickel-base alloy that provides strength and corrosion resistance in a variety of environments [1]. Its wide use in the aerospace, marine, chemical, and petrochemical applications is due to a good combination of yield strength, creep strength, excellent fabricability, weldability, and good resistance to high-temperature corrosion [2]. The high content of Cr and Mo provides good corrosion resistance, while Fe and Nb provide solid solution strengthening.

Additive manufacturing is the process in which parts are fabricated in a layer-by-layer format. Freedom of design, rapid prototyping, mass customization, fabrication of complex geometries, and part count consolidation are some of the benefits that additive manufacturing provides [3]. As per ISO/ASTM 52900, powder bed fusion (PBF) is a process category in which thermal energy, delivered by a laser or electron beam, selectively fuses regions of a powder bed. In the EB-PBF systems, the energy source is an electron beam generated by thermionic emission from a tungsten filament. Metallic materials that are commonly fabricated using EB-PBF systems include Ti-6Al-4V, titanium aluminide (TiAl), nickel alloys, high alloy tool steels, stainless steels, cobalt-chrome alloys (CoCr), and copper [4].

Alloy 625 is a good candidate to be manufactured by Electron Beam Powder Bed Fusion (EB-PBF), reaching nearly fully dense parts ($\approx 99.5\%$) in previous studies [5][6]. The fabrication of Alloy 625 through Electron Beam Powder Bed Fusion (EB-PBF) additive manufacturing has not been extensively reported in the literature. Therefore, this project serves the purpose of enriching the information on the additive manufacturing, microstructure, and mechanical performance of EB-PBF fabricated Alloy 625.

Firstly, printing process parameters were developed to build Alloy 625 through EB-PBF by varying speed function (a measure of the beam scan speed), focus offset (a measure of the beam spot size), and observing surface finish, part skeletal density, and part internal porosity to achieve nearly fully dense parts. The hardness and tensile strength of additively manufactured Alloy 625 have been reported to exceed those of wrought parts, but their ductility is low [7]. Therefore, printed tensile specimens were heat-treated to enhance part density, homogenize the microstructure, and increase the ductility of the printed specimens. This heat treatment involved stress relieving, hot isostatic pressing (HIP), and solution treatment. Murr et al. reported that a hot isostatic pressing heat treatment dissolved the columnar precipitates observed in the as-built form of EB-PBF Alloy 625 parts and recrystallized the columnar grains into a nearly equiaxed grain structure. This change in the microstructure induced an increase in elongation, but a reduction in hardness and tensile strength [6]. Finally, mechanical properties and microstructure of the printed Alloy 625 parts were analyzed in terms of build direction (horizontal vs. vertical) and condition (as-built vs. heat-treated).

1.1 Motivation

To report successful fabrication of Alloy 625 and analyze the mechanical behavior of printed parts subjected to stress-relieving, HIP, and solution heat treatment. Expand on machine set-up and parameter development for fabrication of Alloy 625 on EB-FPBF systems.

1.2 Thesis Objectives

- Derive process parameters leading to a nearly fully dense part and smooth top part surface finish avoiding visible over-melting or porosity.

- Characterize as fabricated and heat-treated Alloy 625 microstructures, and mechanical properties (yield strength, ultimate tensile strength, elongation, modulus of elasticity, and hardness).
- Compare the mechanical properties and microstructures of as-built and heat-treated tensile coupons printed vertically and horizontally.

PREVIEW

CHAPTER 2: LITERATURE REVIEW

Additive manufacturing (AM) is the process by which an object is built layer-by-layer directly from digital data created using computer-aided design. Additive manufacturing divides into seven process categories depending on the method employed to join the layers of material together. According to ISO/ASTM 52900, these seven process categories are: binder jetting, directed energy deposition, material extrusion, material jetting, sheet lamination, vat photopolymerization, and powder bed fusion [8].

2.1 Binder Jetting

As per ISO/ASTM 52900, binder jetting is an additive manufacturing process in which a liquid bonding agent is selectively deposited to join powder materials. Binder jetting was first invented by Sachs et al. in 1989 at the Massachusetts Institute of Technology [9][10]. In this process, an inkjet print head is used to deposit the liquid bonding agent over a thin layer of powder to form the desired pattern per layer. Then, the build platform is lowered, and a new layer of powder is spread on top of the glued pattern with the use of a roller or blade [11]. The process is repeated until the 3D part is produced. A schematic of the binder jetting process is shown in Figure 1. The produced part is then cured or “dried” to harden the material and allow the removal of excess powder [12]. The glued part, often called “green body” is taken through a sintering cycle to burn off the polymer binder and sinter metal particles together, which results in part shrinkage [13]. Finally, to improve density and strength, the part may be infiltrated with a lower-melting point metal as in [14].

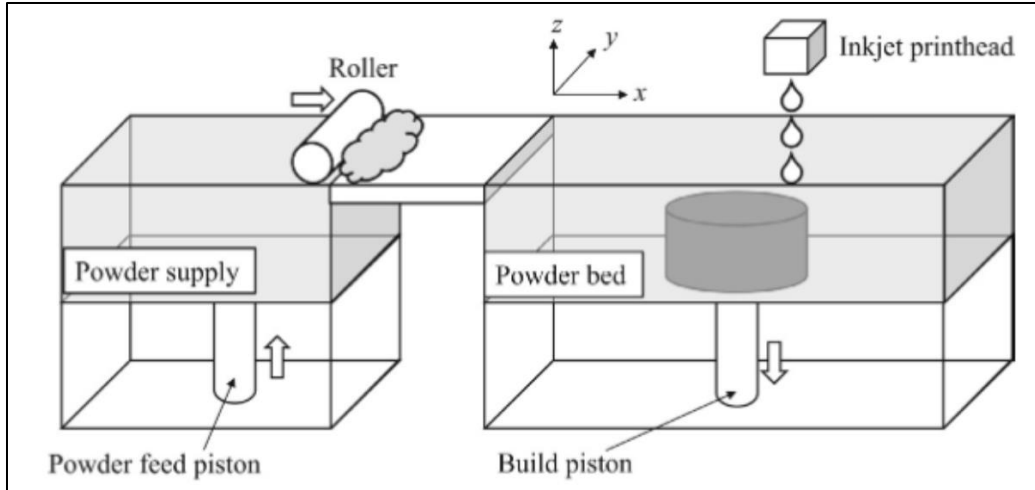


Figure 1. Schematic of binder jetting three-dimensional printing technology [13].

2.2 Directed Energy Deposition

As per ISO/ASTM 52900, directed energy deposition (DED) is an additive manufacturing in which focused thermal energy is used to fuse materials by melting as they are being deposited. In these systems, the energy source can be a laser, electron beam, or plasma arc; and the feedstock material used may also vary among metal powder or wire [15]. Some common metals that have been printed with this technology include titanium, aluminum, stainless steel, and copper [16][17]. Figure 2 shows the schematics of two directed energy deposition (DED) systems; (A) uses a laser as the energy source and powder feedstock and (B) uses an electron beam as the energy source and wire feedstock [15]. Electron beam DED systems require a vacuum-controlled environment, while laser DED systems employ other methods to introduce a shielding inert gas blown together with the powder feedstock [15][18]. Additionally, it has been reported that powder DED systems may use multiple nozzles to eject metal powders, which allows the user to mix different materials and produce functionally graded materials [15][19][20][21]. Moreover, this technology is often used to repair or add material to existing parts [16][22].

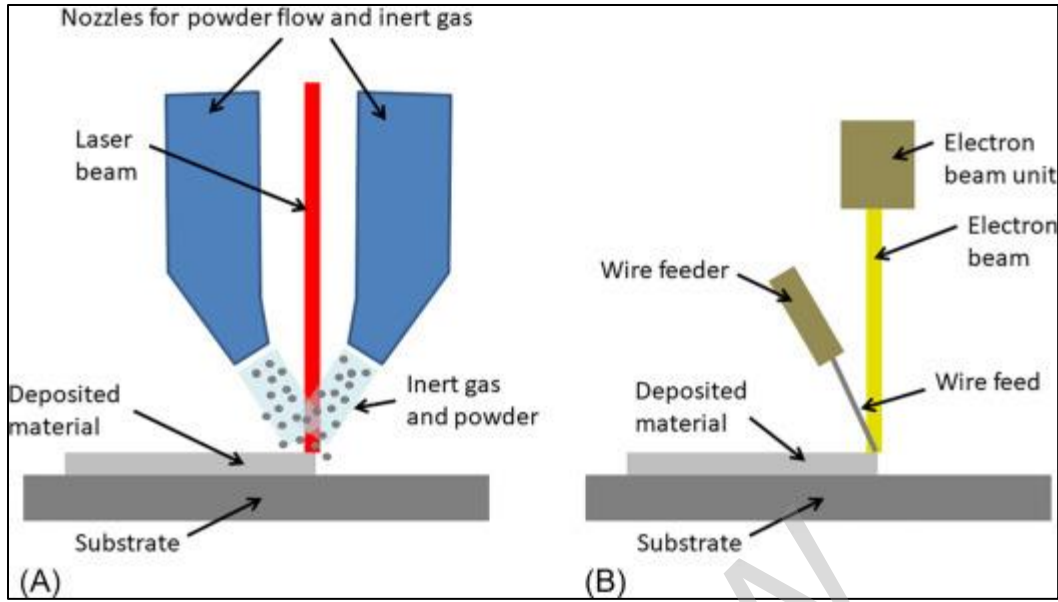


Figure 2. Schematics of two DED systems (A) uses laser together with powder feedstock and (B) uses electron beam and wire feedstock [15].

2.3 Material Extrusion

As per ISO/ASTM 52900, material extrusion is an additive manufacturing process in which material is selectively dispensed through a nozzle or orifice. Material extrusion is a common technology used to print thermoplastics, whose applications vary from recreational prints, engineering prototypes, and functional parts and systems [23]. Some examples of thermoplastics that can be used in this process include acrylonitrile butadiene styrene, polylactic acid, polycarbonate, thermoplastic polyurethane, and aliphatic polyamides (nylon) [11]. The common setup of a material extrusion printer includes a liquefier head, extrusion nozzles, and a build platform as shown in Figure 3. In summary, the heated material is fed in the extrusion nozzle and deposited on the build platform layer by layer. Usually, during this layer-by-layer process, the build platform moves vertically, while the extrusion head moves in x-y directions [24][11]. One important observation in this process is that the filament deposition pattern per layer and part

orientation are both important factors for the mechanical performance of printed parts as previously studied in [25][26][27][28][29].

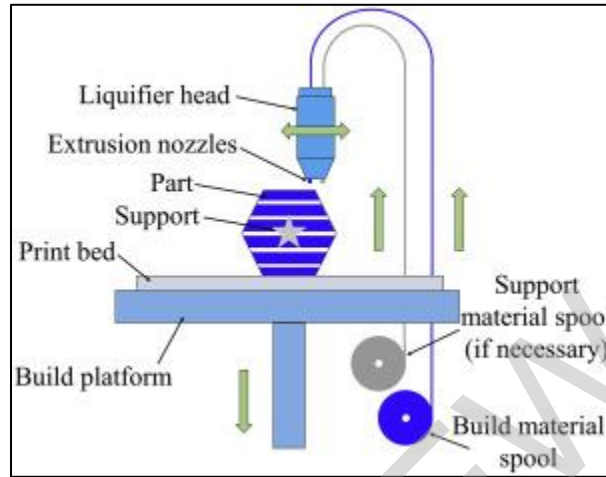


Figure 3. Schematic of the material extrusion process [11].

2.4 Material Jetting

As per ISO/ASTM 52900, material jetting is an additive manufacturing process in which droplets of build material are selectively deposited. This technology was developed by Objet Geometries in 2000, and it was acquired by Stratasys in 2012 [30][31]. A common schematic for the material jetting process is shown in Figure 4, which includes components such as print heads, ultraviolet (UV) curing lamp, leveling blade, and a moving platform. Once the photopolymer material is selectively deposited, UV light is emitted onto the molten material for curing [30][32]. The UV light source used in material jetting printers has a wavelength range of 190-400 nm [32][33][34]. After curing each layer, the platform is lowered by a previously established layer thickness, and a new layer of material is jetted onto the previous layer. This process is repeated until a 3D part is complete. Overhanging features require the use of support structures, which can

be subsequently removed through sonication, heating, or with the use of a high-pressure water jet [30][35].

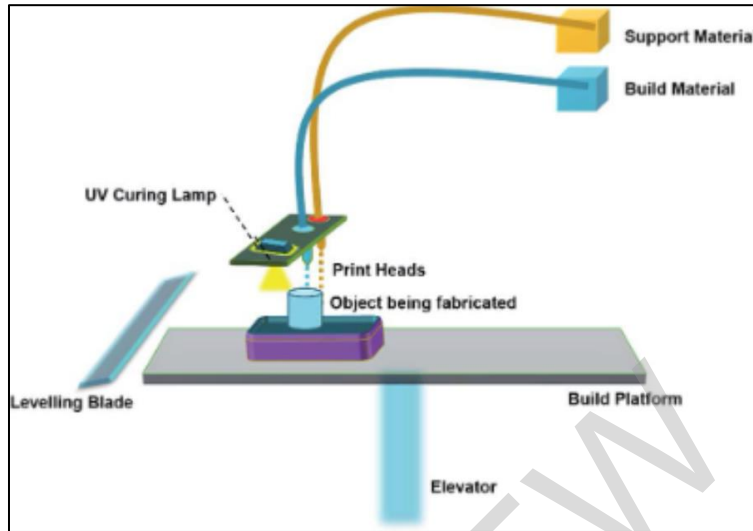


Figure 4. Schematic of the material jetting process [30].

2.5 Sheet Lamination

As per ISO/ASTM 52900, sheet lamination is an additive manufacturing process in which sheets of material are bonded to form an object. This technology was first developed by Helysis Inc. [36]. A common setup in a sheet lamination process includes a sheet of paper coated with a thermoplastic adhesive, which is then bonded to the previous layer with the use of a heated roller. Subsequently, a CO₂ laser cuts the desired pattern, and this process repeats until the 3D part is complete [37]. A schematic of the described process is shown in Figure 5. In other variations of the sheet lamination process metallic sheets are used as feedstock material and they are stacked together by employing an ultrasonic or laser localized energy source [13][38]. A technique called ultrasonic additive manufacturing (UAM) or ultrasonic consolidation (UC) consists of applying an ultrasonic wave and mechanical pressure on pre-cut sheet metal attacks at room temperature, which bonds the layers by diffusion [39][40].

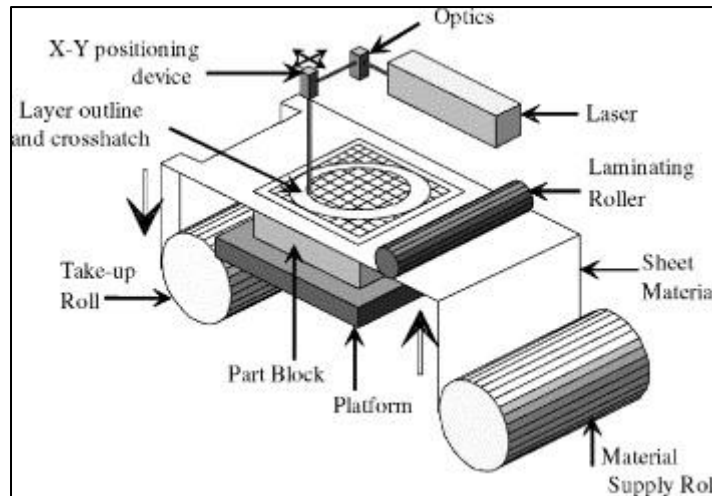


Figure 5. Schematic of sheet lamination process [37].

2.6 Vat Photopolymerization

As per ISO/ASTM 52900, vat photopolymerization is an additive manufacturing process in which liquid photopolymer in a vat is selectively cured by light-activated polymerization. The polymerization process consists of using visible or ultraviolet (UV) light to cure a photopolymer material stored in a vat layer by layer [41]. The curing light initiates the polymerization reaction by forming chains of polymers to form a solid resin, which cannot return to liquid form [41][42][43][44][45]. As mentioned in Pagac et al. [41] vat photopolymerization is classified in different categories depending on the energy source used to cure the photopolymers. For example, stereolithography (SLA) uses lasers, and digital light processing (DLP) utilizes a digital light projector [46][47]. The common setup of an SLA machine is shown in Figure 6.